

Thermal conductivity of geomaterial foams based on silica fume

J. Bourret · E. Prud'homme · S. Rossignol ·
D. S. Smith

Received: 4 November 2010 / Accepted: 19 July 2011 / Published online: 30 July 2011
© Springer Science+Business Media, LLC 2011

Abstract Porous materials have been prepared from a solution containing sodium silicate and sodium hydroxide with the addition of silica fume. Kaolin and diatomite were also tested as additives to the initial formulation. This method yields consolidated geomaterial foams without requiring thermal treatment above 50 °C. The influence of chemical composition on the thermal conductivity was studied. The choice of raw materials was found to play an important role. The accuracy of thermal conductivity measurements was evaluated by comparing the steady state heat flow method with the laser flash technique for five different reference materials giving values within 6%. Using the steady state heat flow method, a value of $0.12 \pm 0.01 \text{ W m}^{-1} \text{ K}^{-1}$ was then obtained for consolidated foams, made with kaolin as the precursor, containing approximately 70% of porosity.

Introduction

The development of highly performant thermal insulators is a major issue in the field of high temperature processing and equipment as well as in the building sector. Furthermore, thermally insulating materials based on fibers or loosely compacted fine particles are being progressively phased out because of hygiene and safety regulations imposed in the European community.

Alternative materials with a very low thermal conductivity ($<0.1 \text{ W m}^{-1} \text{ K}^{-1}$) are the object of modern research. Creation of porosity is the main issue in the development of new insulating materials. Indeed, air has a very low value of thermal conductivity ($0.026 \text{ W m}^{-1} \text{ K}^{-1}$).

A porous solid can be assimilated to a two-phase system constituted by the solid skeleton and air. Collishaw and Evans [1] have reviewed different analytical expressions describing the effective thermal conductivity of the porous solid as a function of pore volume fraction. In each case, there is a geometrical simplification of the microstructure taking into the account the spatial distribution of the phases. These theoretical models can be used to assess the potential and limits of different approaches for the preparation of thermal insulators. Knowledge of the solid phase thermal conductivity and the pore size distribution are therefore key input parameters [2].

To prepare a porous material, different methods are possible, such as application of a limited thermal treatment to a pressed powder compact, formation of foams with infiltration of a polymer preform [3], or use of a pore-forming agent [4]. For economic and environmental considerations, geomaterials synthesized from aluminosilicate natural raw materials provide an interesting alternative. Previous study has already shown the possibility of synthesizing geomaterial foam based on metakaolin or kaolin and potassium silicate [5]. Their high pore volume fraction leading to the designation of foam is due to production of molecular hydrogen from a chemical reaction involving free silicon contained in the precursors.

The aim of this study is to determine the feasibility of making geomaterial foams based on different raw materials and to investigate their insulating properties. In particular, less expensive sodium silicate has been used instead of

J. Bourret (✉) · E. Prud'homme · S. Rossignol · D. S. Smith
Groupe d'Etude des Matériaux Hétérogènes, CEC,
12 rue Atlantis, 87068 Limoges, France
e-mail: julie.bourret@etu.unilim.fr

D. S. Smith
e-mail: david.smith@unilim.fr

potassium silicate and in some formulations, kaolin has been totally replaced by diatomite, a natural porous material or removed.

For characterisation of the thermal conductivity of these materials, the laser-flash technique yields data of questionable value when the typical pore dimension is greater than 1 mm compared to a sample thickness of less than 3 mm. A steady state heat flow method has therefore been used. Validation of these measurements was thus made by comparing the values obtained with the two techniques for well-known insulators. Finally the thermal conductivity measurements for the new materials were analyzed using standard relations such as the Maxwell–Eucken model in order to obtain effective values for the solid skeletons.

Materials and methods

Preparation of the geomaterial foams

The geomaterials are synthesized from a reactant mixture including a basic medium, silica fume, and an optional additive, using the protocol given in Fig. 1.

The basic medium is prepared from NaOH pellets dissolved in commercial sodium silicate ($\text{Si}/\text{Na} = 1.7$, 59 wt% H_2O). The silica fume is an industrial by-product, supplied by Ferropem (France) and presents the particularity of containing a small amount of free silicon. The optional additives which substitute for a part of the silica fume are a kaolin clay supplied by IMERYS and diatomite (Primisil[®] KN25 supplied by AGS), a natural porous material (Fig. 2).

The obtained reactive mixture is placed in a polyethylene mold in an oven at 50 °C for 24 h. The different formulations which were prepared in this work are presented in Table 1.

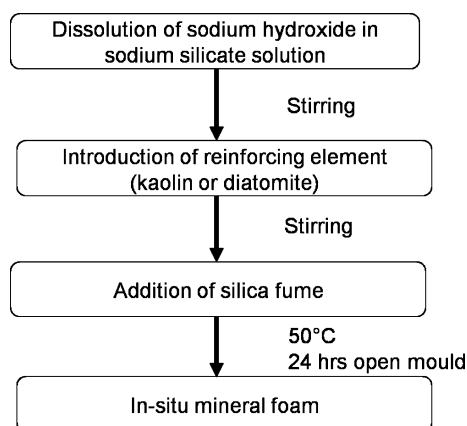


Fig. 1 Synthesis protocol of consolidated mineral foam

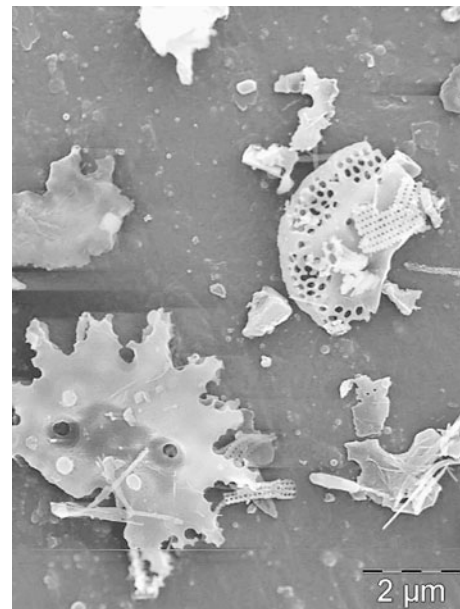
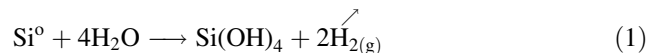


Fig. 2 SEM micrograph of diatomite powder

During mixing, the silicon contained in silica fume is oxidized by water in the alkali medium leading to the formation of $\text{Si}(\text{OH})_4$ species and molecular hydrogen [5] according to the reaction:



The foam formation is then due to the combination of three phenomena, the production of molecular hydrogen, an increase of viscosity due to treatment at 50 °C and the consolidation of material. The last two mechanisms trap molecular hydrogen to form bubbles leading to creation of the porosity.

Structural and morphological characterization

To characterize the porosity of the foams obtained, the software image analysis package Image J was used. The machined samples for measurement of thermal conductivity

Table 1 Formulations of the different foams

| Sample label | Sodium hydroxide (wt%) | Sodium silicates (wt%) | Additive (Ka, Di or SF _{ad}) (wt%) | SF (wt%) | $\frac{\text{Mass}_{\text{alkali}} + \text{SF}}{\text{Mass}_{\text{additive}}}$ |
|-----------------------|------------------------|------------------------|--|----------|---|
| SF _{ad} _2.7 | 8.43 | 43.57 | 27.39 | 20.61 | 2.7 |
| Ka_2.7 | 8.43 | 43.57 | 27.39 | 20.61 | 2.7 |
| Ka_5.3 | 9.77 | 50.49 | 15.87 | 23.88 | 5.3 |
| Di_2.7 | 8.43 | 43.57 | 27.39 | 20.61 | 2.7 |
| Di_5.3 | 9.77 | 50.49 | 15.87 | 23.88 | 5.3 |

Ka kaolin, *Di* diatomite, *SF_{ad}* Silica fume, *Sample label* additive_ $\frac{\text{Mass}_{\text{alkali}} + \text{SF}}{\text{Mass}_{\text{additive}}}$

(3 cm square blocks) of thickness approximately equal to 2 mm are photographed. The photographs are set into two colors by adjusting the brightness and contrast. The phases of the material matrix and pores appear. The functions of the software can then measure the area of the pores and calculate the related percentage and size distribution with respect to the image area. According to statistical considerations, this percentage corresponds to pore volume fraction of the sample in both two and three dimensions. Three images of the same sample were analyzed to check for reproducibility. The morphology of the foams was examined at higher magnification using scanning electron microscopy (SEM). Prior to their observation, a platinum layer was deposited on the samples.

Thermal characterization

Equipment

Thermal conductivity measurements of the geomaterial foams were made with a simple steady state heat flow apparatus operating at room temperature (supplied by CAPTEC, France). Samples are prepared in the form of squares blocks : $30 \times 30 \text{ mm}^2$ with a thickness varying from 1 to 5 mm. It should be noted that the samples for measurements are cut out of the core of the geomaterial foam block. The heat source is adjusted so that a temperature difference ΔT of approximately 5°C is imposed across the sample which is measured precisely with a differential thermocouple. The resulting average heat flow (ϕ_{av}) through the sample is evaluated using thermoelectric heat flux sensors to assess the incoming and outgoing heat flows. The apparent thermal resistance (R) of a sample is then calculated using the relation:

$$R = \frac{\Delta T}{\phi_{av}} = \frac{e}{\lambda} + R_{contacts} \tag{2}$$

where e is the sample thickness and $R_{contacts}$ represents the total resistance of the contacts of the sample to the copper plates of the sample holder [6]. This contribution to apparent thermal resistance can be eliminated by measuring several samples of different thicknesses. Least squares

linear regression is then used on the experimental data plotted in the form of thickness versus apparent thermal resistance to calculate the value of thermal conductivity λ from the slope.

The laser flash method was also used to measure the thermal diffusivity α on disc samples with dimensions 12 mm in diameter and 2 mm in thickness [7]. Samples were coated with a thin graphite layer to improve absorption of the laser beam and the emission of the thermal signal from the near face. The temperature–time data were analyzed by Degiovanni’s method [8] which takes into account the effect of heat losses on the value of thermal diffusivity. The thermal conductivity of the sample is then calculated with the relation:

$$\lambda = \alpha \cdot C_p \cdot \rho \tag{3}$$

where C_p is the specific heat capacity and ρ is the density.

Validity of thermal conductivity measurements

Highly insulating materials with values of thermal conductivity less than $0.2 \text{ W m}^{-1} \text{ K}^{-1}$ push the measurement techniques to the limit of their range. In order to check the validity of our measurements, a study of five insulating reference materials was made. These were perspex, xonotlite, isofrax insulator, supplied by Unifrax (France), cork, and expanded polystyrene. To avoid damaging the detector, laser flash measurements were not made on perspex because it is transparent or on polystyrene because it is translucent. The cork and xonotlite are characterized by large mm sized pores. For each material, three disc samples were cut for the laser flash measurements and three sets of three samples of different thicknesses were used for the steady state heat flow method. Standard deviation values give a useful representation of the uncertainty. Table 2 compares values obtained by the two techniques with reference values.

In fact, perspex is used as the standard for calibration of the heat flow method. For xonotlite, isofrax insulator, and cork, the two techniques yield similar values with the maximum discrepancy being 21%, possibly related to a certain heterogeneity in the xonotlite with the presence of

Table 2 Comparison of thermal conductivity measurements by the steady state heat flow method and the laser flash technique with reference values for five different materials

| Material | $\lambda_{reference}$ ($\text{W m}^{-1} \text{ K}^{-1}$) | $\lambda_{measured}$ ($\text{W m}^{-1} \text{ K}^{-1}$) | | Standard deviation (%) | |
|-------------|---|---|-----------------------|------------------------|-----------------------|
| | | Heat flow method | Laser flash technique | Heat flow method | Laser flash technique |
| Perspex | 0.190 | 0.190 | – | 5.2 | – |
| Xonotlite | 0.120 | 0.102 | 0.126 | 1.0 | 21 |
| Isofrax | 0.047 | 0.069 | 0.073 | 0.4 | 21 |
| Cork | 0.045 | 0.066 | 0.061 | 1.7 | 5.2 |
| Polystyrene | 0.040 | 0.047 | – | 2.9 | – |

Standard deviations for measurements

large mm sized pores. We remark that the steady state heat flow method can be used to measure thermal conductivity values down to $0.05 \text{ W m}^{-1} \text{ K}^{-1}$ within 6%. This is the preferred method for characterizing the geomaterial foams which can contain mm sized pores. The equivalent thermal conductivity of the very porous material then refers to the material contained between the planes defined by the copper plates and includes the pore volume fraction.

Results

Morphology of geomaterial foams

The five different geomaterial foam formulations are very porous. Their pore volume fractions varied from 0.60 to 0.67 (Table 3). The corresponding pore morphologies for each formulation are shown in Fig. 3 and are generally large equiaxed roughly spherical inclusions. These, however, varied in size from 0.2 to 5 mm depending on the formulation. In fact, a second population of smaller pores ($<0.1 \text{ mm}$) could be identified in the apparently solid skeleton (Fig. 4). For each sample, the relative proportion of this size range is indicated in Table 3.

Thermal conductivity values

Thermal conductivity measurements (λ_{eff}) are given in Table 3. Examining these results, two groups of values could be distinguished. Indeed foams based on kaolin have a thermal conductivity less than $0.17 \text{ W m}^{-1} \text{ K}^{-1}$ whereas those containing diatomite or silica fume precursors exceed $0.2 \text{ W m}^{-1} \text{ K}^{-1}$. The measurement uncertainty can be estimated at $\pm 0.01 \text{ W m}^{-1} \text{ K}^{-1}$, implying the difference is significant. Given that the pore volume fractions are rather similar, this difference can be explained by variation of chemical composition and/or pore size distribution. Because of the H_2 production in the reaction mechanism involved in their formation, it is indeed not possible to prepare monolithic materials of the same composition as

the foams. Consequently an estimate is made using a model which takes into account the effect of porosity.

Comparison of solid phase thermal conductivity

Two standard models can be considered which describe the thermal conductivity of a porous solid. For open porosity, Landauer's effective medium expression has given close agreement to experimental data for alumina ceramics upto pore volume fractions of 0.6 but then significant difference between theory and experiment is observed for higher pore volume fractions [9]. For the present set of samples, the approach would tend to overestimate the solid phase thermal conductivity. Given the cellular nature of the microstructures, shown in Fig. 3, a model describing the effect of closed porosity on thermal conductivity seems more appropriate.

As a first approach, Maxwell–Eucken's expression can be used to predict the thermal conductivity of a solid containing unconnected spherical pores [10]. This can be re-expressed in terms of λ_s , the calculated solid phase conductivity with:

$$\lambda_s = \frac{\lambda_{\text{eff}}(2 + v_p) - \lambda_p(1 + 2v_p)}{4(1 - v_p)} + \frac{\sqrt{[\lambda_p(1 + 2v_p) - \lambda_{\text{eff}}(2 + v_p)]^2 + 8\lambda_{\text{eff}}\lambda_p(1 - v_p)^2}}{4(1 - v_p)} \quad (4)$$

where λ_{eff} is the foam thermal conductivity, λ_p is the thermal conductivity of the pore phase, and v_p is the pore volume fraction. The corresponding values which vary from 0.40 to $0.75 \text{ W m}^{-1} \text{ K}^{-1}$ are given in the sixth column of Table 3.

As a second approach, to take into account the pore size distribution, the thermal conductivity of the solid skeleton is calculated in two steps. The material is considered as a system of two phases: large isolated pores ($>0.1 \text{ mm}$) and a pseudo phase containing the solid skeleton and a connected network of smaller pores ($<0.1 \text{ mm}$). The thermal

Table 3 Pore volume fraction and thermal conductivity measurements (λ_{eff}) for five geomaterial foams

| Sample label | Porosity (%) | $\frac{\text{Porosity}_{<0.1\text{mm}}}{\text{Porosity}}(\%)$ | λ_{eff} ($\text{W m}^{-1} \text{ K}^{-1}$) | Standard deviation (%) | λ_s ($\text{W m}^{-1} \text{ K}^{-1}$) | $\lambda_{s'}$ ($\text{W m}^{-1} \text{ K}^{-1}$) |
|----------------------|--------------|---|---|------------------------|--|---|
| SF _{ad_2.7} | 63 | 65 | 0.21 | 0.5 | 0.67 | 1.07 |
| Ka_2.7 | 60 | 50 | 0.17 | 4.2 | 0.45 | 0.58 |
| Ka_5.3 | 67 | 53 | 0.12 | 0.9 | 0.40 | 0.59 |
| Di_2.7 | 63 | 50 | 0.23 | 0.9 | 0.74 | 1.04 |
| Di_5.3 | 62 | 38 | 0.24 | 5.8 | 0.69 | 0.86 |

λ_s and $\lambda_{s'}$ are estimated values of the thermal conductivity of the solid skeleton assuming respectively unconnected spherical pores and then a mixture of large unconnected pores with smaller connected pores

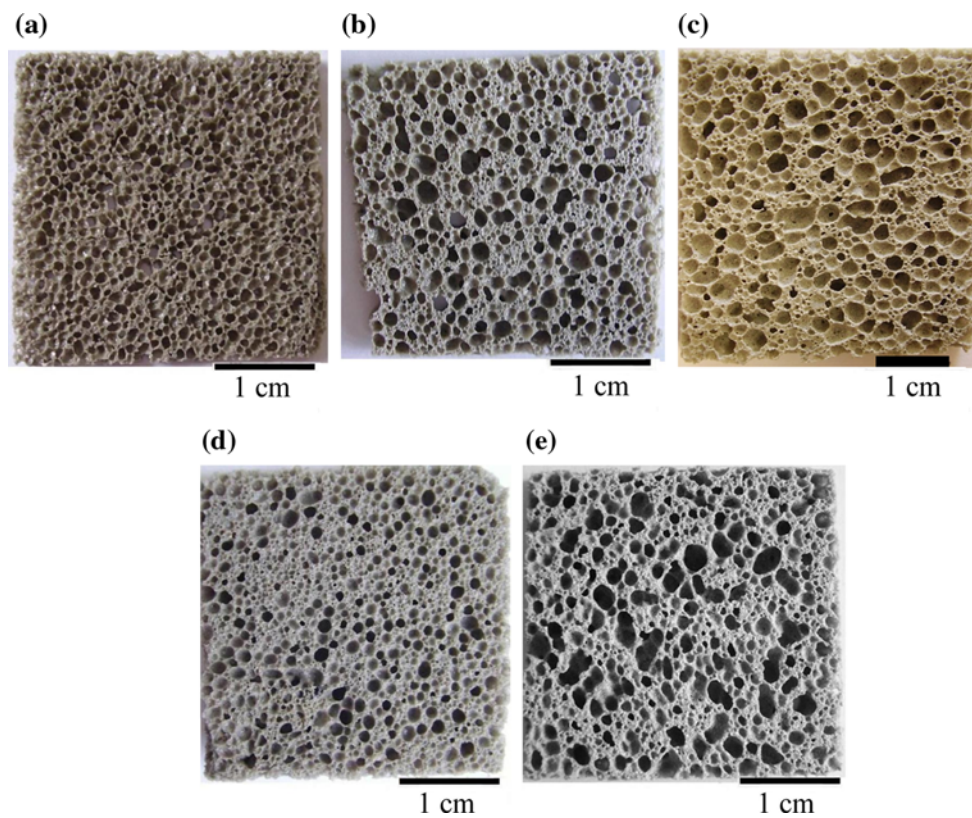


Fig. 3 Sections of foams made from different chemical formulations

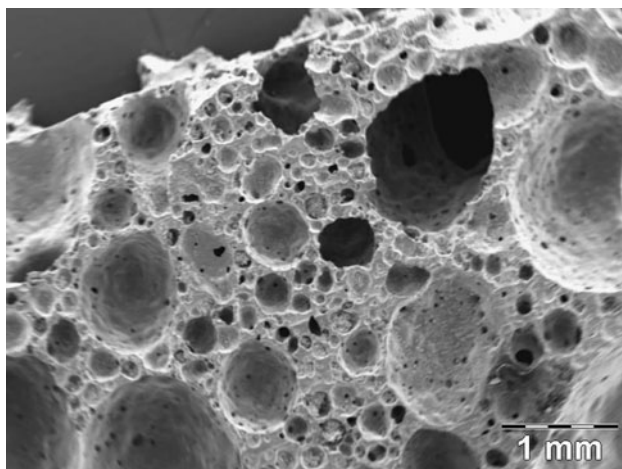


Fig. 4 SEM micrograph example of a kaolin foam (Ka_2.7)

conductivity of the pseudo phase (λ_2) is first calculated using the Maxwell–Eucken approach with Eq. 4. Then to remove the influence of the interconnected smaller pores (<0.1 mm) from the value of λ_2 , a new value $\lambda_{s'}$ corresponding to the thermal conductivity of the solid skeleton is determined using Landauer’s expression [11]. This has been re-expressed in the form :

$$\lambda_{s'} = \frac{2\lambda_2^2 - \lambda_2\lambda_p(3v_{p'} - 1)}{\lambda_p + \lambda_2(2 - 3v_{p'})} \tag{5}$$

where λ_2 is the thermal conductivity of the pseudo phase and $v_{p'}$ is the relative pore volume fraction of the smaller pores (<0.1 mm) in the pseudo phase. The calculated values are given in the seventh column of Table 3 and show a 30–40% increase compared to the one step Maxwell–Eucken values. In fact, the bimodal pore size distribution leads to a noticeable decrease of the effective thermal conductivity of these materials. However, Table 3 also indicates that the difference between the values of thermal conductivity of the two groups of materials, identified in “**Thermal conductivity values**”, is more pronounced in terms of the solid skeleton.

Foams with kaolin precursor exhibit a solid phase conductivity less than $0.6 \text{ W m}^{-1} \text{ K}^{-1}$ whereas the foams with diatomite or additional silica fume yield values close to $1 \text{ W m}^{-1} \text{ K}^{-1}$. This difference implies that the chemical composition has a significant influence on the thermal conductivity of the foams. X-ray diffraction patterns revealed that all the foams have an amorphous phase. The values of thermal conductivity for the solid skeleton containing diatomite or additional silica fume can be compared

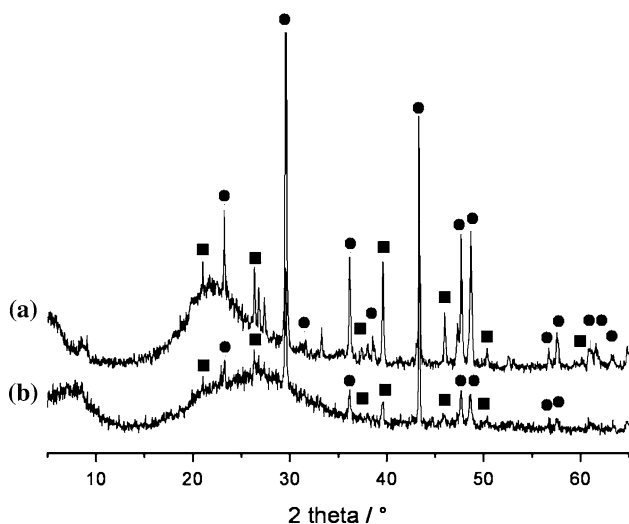


Fig. 5 Diffractograms of the diatomite powder (a) and of the foam Di_5.3 (b). The two crystalline phases are quartz (04-008-7653) (filled square) and calcite (01-089-1305) (filled circle)

to typical values of thermal conductivity of silica glass ($\approx 1.4 \text{ W m}^{-1} \text{ K}^{-1}$ [12]).

To examine this point further, the XRD pattern of the diatomite powder and that of the foam Di_5.3 are presented in Fig. 5. The dome located between 15° and 28° , centered at 22° , reveals the presence of an amorphous phase in the diatomite powder among crystalline phases of quartz and calcite. In the XRD pattern of the foam based on diatomite, the dome maximum shifts to 26° . This is explained by a higher disorder of raw materials in a new type of amorphous phase. In addition small peaks corresponding to residual crystalline phases of quartz and calcite originating from the unreacted diatomite are displayed. The solid phase of the foam is then composed of a mixture of an amorphous phase and crystalline phases.

Conclusion

The low values of thermal conductivity ($< 0.25 \text{ W m}^{-1} \text{ K}^{-1}$) of the different foams confirm the very interesting insulating

properties of these materials close to those of a cellular concrete ($0.16\text{--}0.33 \text{ W m}^{-1} \text{ K}^{-1}$) [13]. Moreover, the nature of the chemical composition of the solid skeleton really influences the solid phase thermal conductivity. With the use of kaolin, a foam was obtained which exhibits a thermal conductivity of $0.12 \text{ W m}^{-1} \text{ K}^{-1}$ with an accuracy of $\pm 0.01 \text{ W m}^{-1} \text{ K}^{-1}$, evaluated with the steady state heat flow method. Future work should investigate the influence of the molar amounts of silicon and aluminum on thermal conductivity as well as the mechanisms of foam formation and porosity control by focusing more closely on the viscosity of mixtures. The aim is to carefully tailor materials with desired thermal and mechanical properties.

Acknowledgement Julie Bourret would like to thank Samir Ben Lakhel for help with the laser flash measurements and the Limousin Region for financial support.

References

- Collishaw PG, Evans JRG (1994) *J Mater Sci* 29:2261. doi: [10.1007/BF00363413](https://doi.org/10.1007/BF00363413)
- Nait-Ali B, Haberko K, Vesteghem H, Absi J, Smith DS (2006) *J Eur Ceram Soc* 26(16):3567
- Bouaziz J, Bouzouita K, Lecompte JP, Saunier S, Jarrige J (2003) *Silic Ind* 11(12):147
- Gregorova E, Pabst W (2007) *J Eur Ceram Soc* 27(2–3):669
- Prud'homme E, Michaud P, Joussein E, Peyratout C, Smith A, Arrii-Clacens S, Clacens JM, Rossignol S (2010) *J Eur Ceram Soc* 30(7):1641
- Hladik J (1990) *Métrieologie des propriétés thermophysiques des matériaux, volume fluxmètres à gradient thermique*. Masson Edition, Paris
- Parker WJ, Jenkins RJ, Butler CP, Abbott GL (1961) *J Appl Phys* 32(9):1679
- Degiovanni A (1977) *Int J Therm Sci* 16(185):420
- Nait-Ali B, Haberko K, Vesteghem H, Absi J, Smith DS (2007) *J Eur Ceram Soc* 27(2–3):1345
- Maxwell JC (1892) *A treatise on electricity and magnetism*. Clarendon Press, Oxford
- Landauer R (1962) *J Appl Phys* 33:3125
- Kittel C (1949) *Phys Rev* 75(6):972
- Kornmann M (2007) *Clay bricks and rooftiles manufacturing and properties*. Société de l'industrie minérale, Paris